

# Machine learning assisted droplet trajectories extraction in dense emulsions and their analysis

Mihir Durve<sup>1</sup>, Adriano Tiribocchi<sup>2</sup>, Andrea Montessori<sup>3</sup>, Marco Lauricella<sup>2</sup>, and Sauro Succi<sup>1,2,4</sup>

<sup>1</sup>Center for Life Nano- & Neuro-Science, Fondazione Istituto Italiano di Tecnologia (IIT), viale Regina Elena 295, 00161 Rome, Italy

<sup>2</sup>Istituto per le Applicazioni del Calcolo del Consiglio Nazionale delle Ricerche, via dei Taurini 19, 00185, Rome, Italy

<sup>3</sup>Dipartimento di Ingegneria, Università degli Studi Roma tre, via Vito Volterra 62, Rome, 00146, Italy

<sup>4</sup> Department of Physics, Harvard University, 17 Oxford St, Cambridge, MA 02138, United States

## Abstract

This work analyzes trajectories obtained by YOLO and DeepSORT algorithms of dense emulsion systems simulated by Lattice Boltzmann methods. The results indicate that the individual droplet's moving direction is influenced more by the droplets immediately behind it than the droplets in front of it. The analysis also provide hints on constraints on writing down a dynamical model of droplets for the dense emulsion in narrow channels.

## 1 Introduction

The last decades have witnessed an impressive rise of machine learning methods, which have profoundly impacted many areas of science, ranging from high energy physics and quantum computation to material design, and have played a vital role in recent milestone discoveries [1, 2]. Many machine learning-based applications are targeted to perform specific tasks such as image recognition, natural language processing, sentiments analysis, and handwriting recognition, to name a few [3, 4, 5, 6], with the aim of improving accuracy, decreasing processing speed, and reducing human efforts to perform tasks that are perceived as mundane or labor intensive. In microfluidics, in particular, they have been used to study shapes and predict transport properties of flowing droplets [7, 8, 9].

Deep neural networks have become one of the fundamental mathematical models for implementing machine learning algorithms [10]. Computer vision is one such application domain that uses deep neural networks to perform essentially two tasks, object recognition and object tracking. For example, a computer vision application connected to a camera observing a traffic junction could easily count the number of cars passing through it and monitor their speed, thus making it a widespread tool for smart traffic management [11].

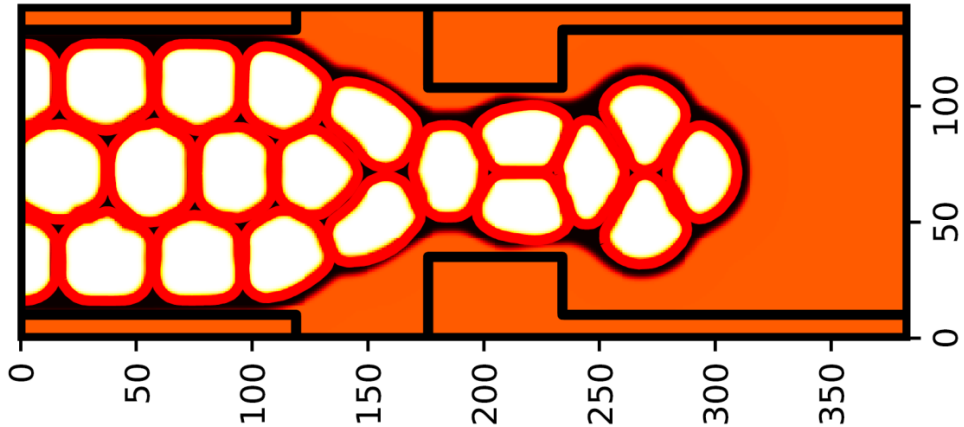


Figure 1: Snapshot of a dense emulsion simulated by Lattice Boltzmann methods.

Recently, we employed two state-of-the-art computer vision algorithms, namely You Only Look Once (YOLO) and DeepSORT, to recognize and track droplets in high internal phase dense emulsions and infer individual droplets trajectories. These emulsions consist of highly ordered liquid droplets arranged in crystal-like structures [12, 13, 14], and have shown promising applications in electrochemical sensing and tissue engineering [15]. Such materials represent a fundamental challenge to non-equilibrium thermodynamics as they feature highly non-Newtonian mechanical and rheological properties. Thus, studying the rich dynamics of these classical many-body systems is crucial to optimize their design as well as the microfluidic devices employed for their synthesis and applications.

In this work, we revisit the tools employed to infer the trajectories of the droplets in dense flowing emulsions simulated using lattice Boltzmann methods, presenting an analysis of such trajectories (obtained via computer vision tools, see Fig.10 and video4.avi in Ref.[16]) in terms of quantities generally adopted to characterize the behavior of active matter systems.

The paper is structured as follows. In the next Section we describe the system under investigation; later in Section 3, we take a brief overview of the computer vision algorithms deployed to get individual droplet trajectories and in Section 4 we present the analysis of the inferred trajectories.

## 2 Physical system

The system under study is a soft granular material made of approximately monodisperse fluid droplets (white region in Fig. 1) immersed within an inter-droplet continuous phase (dark orange lines) and surrounded by an external bulk phase (region outside the emulsion). Its structure closely resembles that of a double emulsion with multi-core morphology [17, 15, 12], where a high volume fraction of dispersed droplets, generally above the close packing limit for spheres, arrange in a tightly packed configuration. This material is produced within a microfluidic channel which, in our system, consists of an inlet reservoir followed by a thinner channel connected to a further downstream reservoir. Further details about the simulations, performed via lattice Boltzmann methods [18, 19, 20], can be found in Ref. [21].

In the next section, we briefly describe the algorithms employed to analyze videos of the

physical system.

### 3 Algorithms

Two algorithms were combined to achieve droplet tracking. The first one, called You only look once (YOLO), is tasked with identifying the droplets in an input image while the second one, called DeepSORT, for tracking the droplets in sequential frames.

#### 3.1 You Only Look Once (YOLO)

YOLO is a single-stage state-of-the-art object detection algorithm. The current version of YOLO (YOLOv5) is the fastest and most accurate object detector on two commonly used, general-purpose object detection datasets called Pascal VOC (visual object classes) [22] and Microsoft COCO object detection datasets [23]. The image analysis speed, i.e. inference speed of the YOLOv5 networks, is at or above 60 frames per second (FPS) [24, 25] for general object detection.

The YOLO algorithm is the fastest due to its smart operating procedure [26, 27]. The input is divided in a  $S \times S$  grid, with each cell responsible for detecting an object within the cell. Each grid cell then predicts  $B$  bounding boxes with their confidence score for each detected object and  $C$  conditional class probabilities for the given object belonging to a specific class. This information is then combined to produce the final output as a single bounding box around the detected object and the class of that object. This final output is then passed to the object tracking DeepSORT algorithm.

The training dataset is used to train the YOLO networks for recognizing the droplets. The training dataset contains several images of droplets and associated label files, which include the location and dimensions of the droplets in each image. The training data is used to get predictions and update the network parameters based on true and predicted output in an iterative process. The technical details of the training procedure to train a YOLO network for droplet recognition is described here [16, 21].

#### 3.2 DeepSORT

The DeepSORT algorithm constructs trajectories of all the detected objects by analyzing sequential frames [28], employing a classical Simple Online Real-Time tracking module [29] in the first stage. This module uses the Hungarian algorithm [30] to distinguish detected objects in two consecutive frames and assigns individual objects their unique identity. The module also uses a Kalman filtering [31] for predicting the future position of the objects based on their current positions. At the second level, the deep network learns object descriptor features to minimize the identity switches as the object moves in subsequent frames. The YOLO and the DeepSORT algorithms together accomplish droplet recognition and tracking, thus allowing to obtain the trajectories of individual droplets (see Fig.10 in Ref. [16]). These ones will be analyzed in the next section.

### 4 Analysis of the droplet trajectories

Preliminary observations (see video4.avi in Ref. [16]) indicate that, in a densely packed configuration, the droplets are moving along the same direction, in a way akin to birds in highly polar flocks [32, 33]. To dig more deeply into such analogy, we compute a polar order parameter  $\psi$

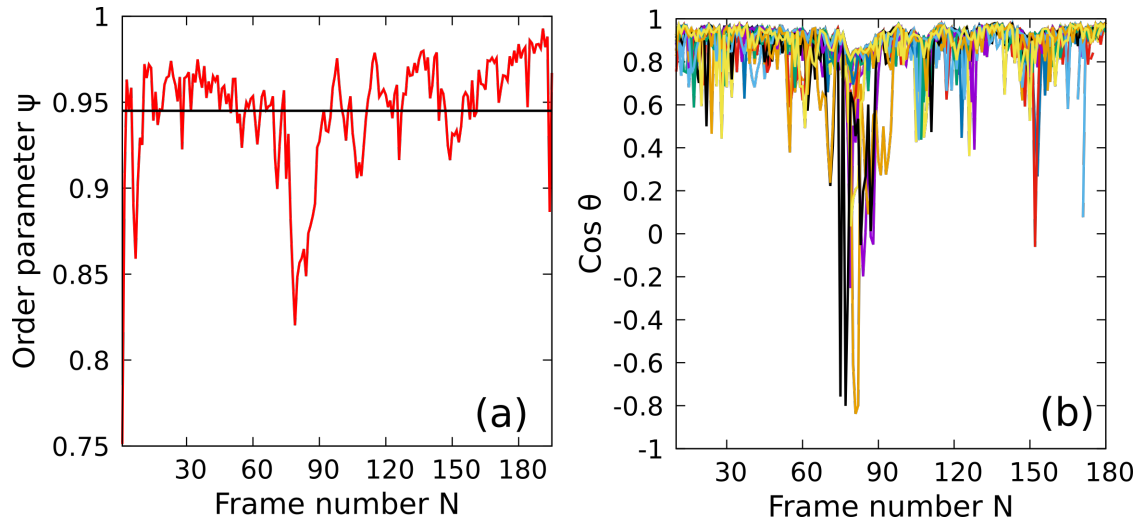


Figure 2: (a) Polar order parameter  $\psi$  computed at each frame. It accounts for moving direction consensus. The black line indicates average of  $\psi$  over all the frames. (b) Cosine of angle between individual droplet's moving direction and average direction of all the droplets. Cosine of the angle computed for individual droplet is shown with a unique color.

which is typically used to measure direction consensus in moving particles [34]. It is computed as

$$\psi = \frac{1}{N} \left| \sum_{i=1}^N \frac{\mathbf{v}_i}{|\mathbf{v}_i|} \right|, \quad (1)$$

where  $N$  is the total number of droplets,  $\mathbf{v}_i$  is the velocity vector of the  $i^{\text{th}}$  droplet and  $|\cdot|$  is the modulus of a vector. If  $\psi = 1$  all the droplets move in the same direction while  $\psi \approx 0$  means that droplets move randomly.

The polar order parameter is shown in Fig. 2(a). The high average value of  $\psi$  ( $\psi > 0.94$ ) indicates that the droplets are moving more or less in the same direction except at a time interval when they are about to enter the narrow channel. In Fig. 2(b), we compare an individual droplet's heading direction with the average moving direction of the emulsion. This comparison is made by measuring the cosine of an angle  $\theta$  between the velocity vector of the emulsion (taken as the resultant velocity vector of all the droplets) and the individual droplet's velocity vector. Except before entering the narrow channel, the droplets move in the direction of their bulk motion as indicated by the cosine value close to unity. In a system containing self-propelled particles (flock of birds, for example), such a high value of polar order parameter and cosine of  $\theta$  corresponds to a highly ordered state in which the agents move in a common direction [32]. These observations show apparent similarities between a flock of birds and the emulsion in terms of dynamical properties. These similarities raise an interesting question, i.e. whether the well-known models [34, 35, 36] to mimic the behavior of active matter systems by taking into account only local interactions can account for the dynamical properties of the emulsion observed here.

Figure 3 shows a scatter-plot of an individual droplet's moving direction with the average direction of its neighbors. The neighbors of a droplet  $i$  are defined as the droplets that are within distance  $R$  from the droplet  $i$  (see Fig. 4) and within the sector of the circle with an

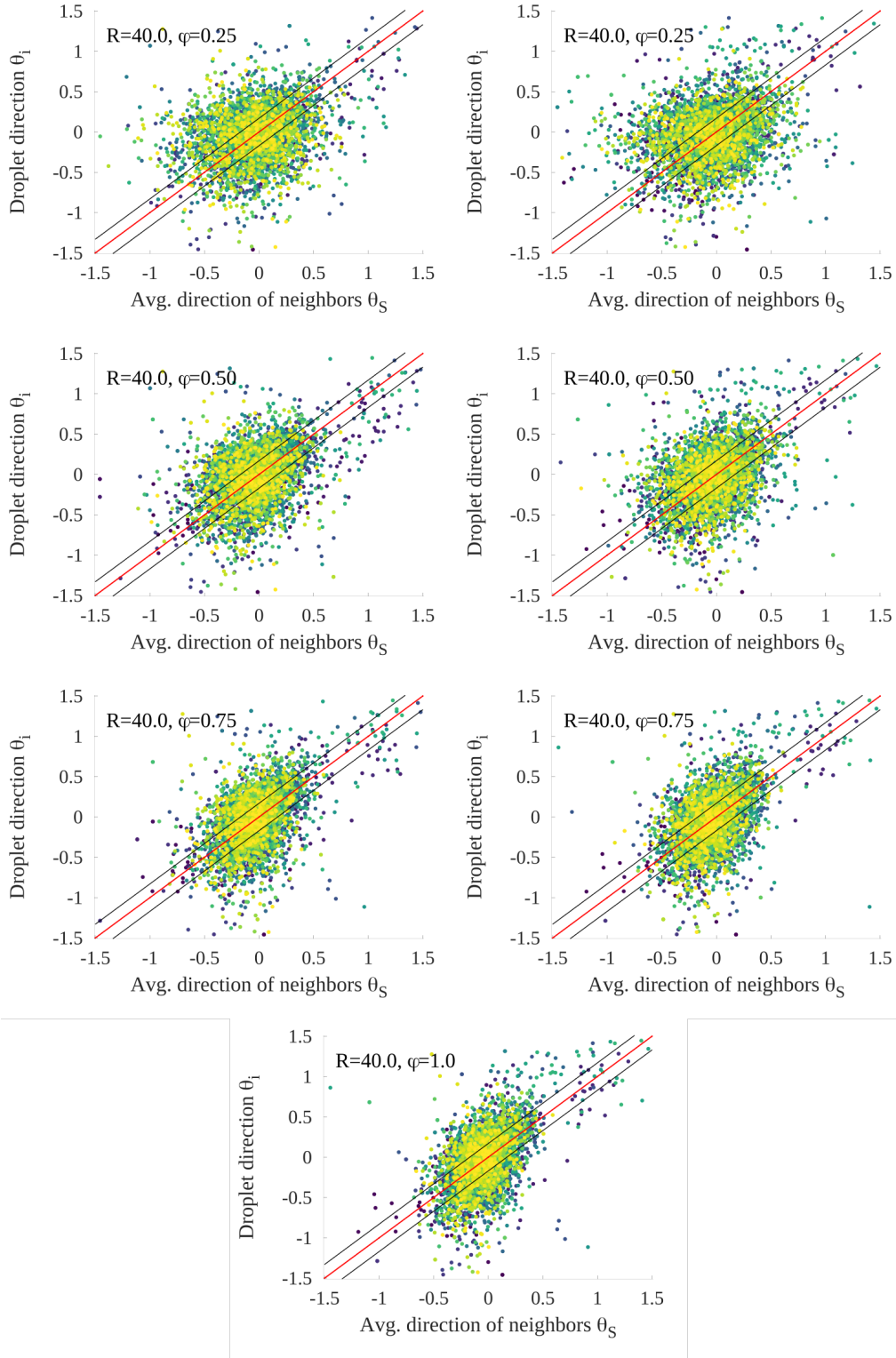


Figure 3: Scatter plot of individual droplet's moving direction and average moving direction of its neighbors. The left column shows neighbor selection in the opposite direction of the motion of the droplet while the right column shows neighbors selected in front of the moving droplet. The middle plot is computed with a full circle with radius  $R$  as the neighborhood of a droplet. The range of  $\phi$  is chosen as  $(0, 1)$ , meaning the actual value of the angle is  $2\pi\phi$ . The points on the red line correspond to the instance when  $\theta_i = \theta_S$ , while points within the two black lines indicate instances where  $\theta_i$  and  $\theta_S$  are within 10 degrees of each other. Thus, points within the band bounded by two black lines show instances when individual droplet's moving direction is approximately same as its neighbors.

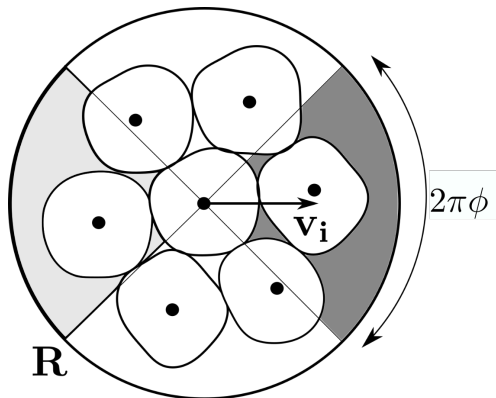


Figure 4: The neighborhood of the droplet  $i$ , placed at the center of a circle of radius  $R$ , is the sector of the circle enclosed by an angle  $2\pi\phi$ . The “front” neighbors are the droplets whose center of mass is within the sector shaded with dark gray color while the “back” neighbors are the ones whose center of mass is within the sector shaded with light gray color. The vector  $\mathbf{v}_i$  is the speed of the droplet  $i$ .

angle  $2\pi\phi$ . The value of  $R$  is chosen such that the circle contains the immediate neighbors of the droplet  $i$ , while the values of  $\phi$  are varied between 0 and 1. We analyzed two cases, one in which the accounted neighbors are in front of the moving droplets, and a further one in which the neighbors are behind the moving droplets. This neighborhood definition allows us to see how these droplets positioned at two different locations affect the motion of an individual droplet  $i$ , an effect that can be inferred by counting the number of instances in which a given droplet is aligned with the average direction of its neighbors. In Fig. 5, we plot the fraction  $F$  of points located within a band indicated by the two black lines of each snapshot of Fig. 3. The points within this band correspond to an instance in which an individual droplet’s moving direction is within ten degrees of its neighbors, i.e.  $|\theta_i - \theta_S| < 0.175$ . Here  $\theta_i$  is the moving direction of droplet  $i$ , and  $\theta_S$  is the moving direction of neighbors of droplet  $i$ . The results show that the droplets are aligned for a comparatively longer time with the droplets behind it rather than the droplets in front of it, thus suggesting that the droplets pushing from behind have higher influence on the individual droplet’s moving direction.

## 5 Conclusions

In this work, we revisit the deep learning-based algorithms to infer the droplet trajectories by analyzing the output of lattice Boltzmann simulation of dense emulsions. We measure various quantities like polar order parameter and deviation of individual droplet’s moving direction with its neighbors. The results suggest that the droplets are aligned for a comparatively longer time with the droplets behind it rather than with the droplets in front of it, meaning that the droplets pushing from behind have higher chance to affect the direction of an individual droplet. It would be interesting to perform similar analysis on data generated by active matter systems in order to further investigate to which extent the analogy with moving emulsions holds and provide further hints to write down a dynamical model of such emulsions in confined systems.

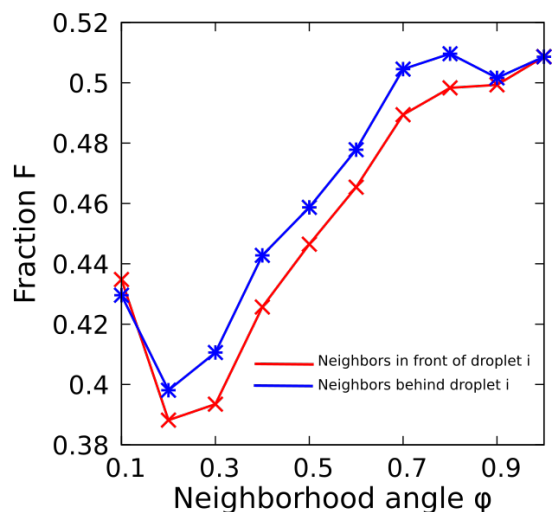


Figure 5: Fraction of instances in which a given droplet is closely aligned with its neighbors as the neighborhood area is varied by changing the angle  $\phi$ .

## 6 Acknowledgments

The authors acknowledge funding from the European Research Council under the European Union’s Horizon 2020 Framework Programme (No. FP/2014-2020) ERC Grant Agreement No.739964 (COPMAT). We gratefully acknowledge the HPC infrastructure and the Support Team at Fondazione Istituto Italiano di Tecnologia.

## References

- [1] Andrew W. Senior, Richard Evans, John Jumper, James Kirkpatrick, Laurent Sifre, Tim Green, Chongli Qin, Augustin Žídek, Alexander W. R. Nelson, Alex Bridgland, Hugo Penedones, Stig Petersen, Karen Simonyan, Steve Crossan, Pushmeet Kohli, David T. Jones, David Silver, Koray Kavukcuoglu, and Demis Hassabis. Improved protein structure prediction using potentials from deep learning. *Nature*, 577(7792):706–710, Jan 2020.
- [2] Giuseppe Carleo, Ignacio Cirac, Kyle Cranmer, Laurent Daudet, Maria Schuld, Naftali Tishby, Leslie Vogt-Maranto, and Lenka Zdeborová. Machine learning and the physical sciences. *Rev. Mod. Phys.*, 91:045002, Dec 2019.
- [3] Darmatasia and M. I. Fanany. Handwriting recognition on form document using convolutional neural network and support vector machines (cnn-svm). *2017 5th International Conference on Information and Communication Technology (ICoICT7)*, pages 1–6, 2017.
- [4] N. H. Tandel, H. B. Prajapati, and V. K. Dabhi. Voice recognition and voice comparison using machine learning techniques: A survey. *2020 6th International Conference on Advanced Computing and Communication Systems (ICACCS)*, pages 459–465, 2020.
- [5] Savita Ahlawat, Amit Choudhary, Anand Nayyar, Saurabh Singh, and Byungun Yoon. Improved handwritten digit recognition using convolutional neural networks (cnn). *Sensors*, 20(12), 2020.

- [6] Kun Han, Dong Yu, and Ivan Tashev. Speech emotion recognition using deep neural network and extreme learning machine. In *Interspeech 2014*, September 2014.
- [7] P. Hadikhani, N. Borhani, S.M.H. Hashemi, and D. Psaltis. Learning from droplet flows in microfluidic channels using deep neural networks. *Scientific Reports*, 9:8114, 2019.
- [8] Yassine Mahdi and Kamel Daoud. Microdroplet size prediction in microfluidic systems via artificial neural network modeling for water-in-oil emulsion formulation. *Journal of Dispersion Science and Technology*, 38(10):1501–1508, 2017.
- [9] Jian Wei Khor, Neal Jean, Eric S. Luxenberg, Stefano Ermon, and Sindy K. Y. Tang. Using machine learning to discover shape descriptors for predicting emulsion stability in a microfluidic channel. *Soft Matter*, 15:1361–1372, 2019.
- [10] Ian Goodfellow, Yoshua Bengio, and Aaron Courville. *Deep Learning*. MIT Press, 2016. <http://www.deeplearningbook.org>.
- [11] Tousif Osman, Shahreen Shahjahan Psyche, J. M. Shafi Ferdous, and Hasan U. Zaman. Intelligent traffic management system for cross section of roads using computer vision. *2017 IEEE 7th Annual Computing and Communication Workshop and Conference (CCWC)*, pages 1–7, 2017.
- [12] Andrea Montessori, Adriano Tiribocchi, Michał Bogdan, Fabio Bonaccorso, Marco Lauricella, Jan Guzowski, and Sauro Succi. Translocation dynamics of high-internal phase double emulsions in narrow channels. *Langmuir*, 37(30):9026–9033, Aug 2021.
- [13] Andrea Montessori, Michele La Rocca, Pietro Prestininzi, Adriano Tiribocchi, and Sauro Succi. Deformation and breakup dynamics of droplets within a tapered channel. *Physics of Fluids*, 33(8):082008, 2021.
- [14] Michał Bogdan, Andrea Montessori, Adriano Tiribocchi, Fabio Bonaccorso, Marco Lauricella, Leon Jurkiewicz, Sauro Succi, and Jan Guzowski. Stochastic jetting and dripping in confined soft granular flows. *Phys. Rev. Lett.*, 128:128001, Mar 2022.
- [15] M. Costantini, C. Colosi, J. Guzowski, A. Barbetta, J. Jaroszewicz, W. Swieszkowski, M. Dentini, and P. Garstecki. Highly ordered and tunable polyhypes by using microfluidics. *J. Mater. Chem. B*, 2:2290–2300, 2014.
- [16] Durve, Mihir, Bonaccorso, Fabio, Montessori, Andrea, Lauricella, Marco, Tiribocchi, Adriano, and Succi, Sauro. Tracking droplets in soft granular flows with deep learning techniques. *Eur. Phys. J. Plus*, 136(8):864, 2021.
- [17] A. S. Utada, E. L. Lorenceau, D. R. Link, P. D. Kaplan, H. A. Stone, and D. A. Weitz. Monodisperse double emulsions generated from a microcapillary device. *Science*, 308:537–541, 2005.
- [18] A Montessori, P Prestininzi, M La Rocca, and S Succi. Lattice boltzmann approach for complex nonequilibrium flows. *Physical Review E*, 92(4):043308, 2015.
- [19] Christophe Coreixas, Bastien Chopard, and Jonas Latt. Comprehensive comparison of collision models in the lattice boltzmann framework: Theoretical investigations. *Physical Review E*, 100(3):033305, 2019.
- [20] S. Succi. *The Lattice Boltzmann Equation: For Complex States of Flowing Matter*. Oxford University Press, 2018.
- [21] Mihir Durve, Fabio Bonaccorso, Andrea Montessori, Marco Lauricella, Adriano Tiribocchi, and Sauro Succi. A fast and efficient deep learning procedure for tracking droplet motion in dense microfluidic emulsions. *Philosophical Transactions of the Royal Society A: Mathematical, Physical and Engineering Sciences*, 379(2208):20200400, 2021.



- [22] The pascal visual object classes homepage. <http://host.robots.ox.ac.uk/pascal/VOC/>.
- [23] Coco dataset homepage. <http://cocodataset.org>.
- [24] Fangbo Zhou, Huailin Zhao, and Zhen Nie. Safety helmet detection based on yolov5. In *2021 IEEE International Conference on Power Electronics, Computer Applications (ICPECA)*, pages 6–11, 2021.
- [25] Luiz Carlos M. Junior and Josã© Alfredo C. Ulson. Real time weed detection using computer vision and deep learning. In *2021 14th IEEE International Conference on Industry Applications (INDUSCON)*, pages 1131–1137, 2021.
- [26] J. Redmon, S. Divvala, R. Girshick, and A. Farhadi. You only look once: Unified, real-time object detection. *2016 IEEE Conference on Computer Vision and Pattern Recognition (CVPR)*, pages 779–788, 2016.
- [27] Joseph Redmon and Ali Farhadi. Yolov3: An incremental improvement. *ArXiv:1804.02767v1*, 2018.
- [28] N. Wojke, A. Bewley, and D. Paulus. Simple online and realtime tracking with a deep association metric. *2017 IEEE International Conference on Image Processing (ICIP)*, pages 3645–3649, 2017.
- [29] Alex Bewley, Zongyuan Ge, Lionel Ott, Fabio Ramos, and Ben Uppcroft. Simple online and realtime tracking. In *2016 IEEE International Conference on Image Processing (ICIP)*, pages 3464–3468, 2016.
- [30] H. W. Kuhn. The hungarian method for the assignment problem. *Naval Research Logistics Quarterly*, 2(1-2):83–97, 1955.
- [31] R. E. Kalman. A New Approach to Linear Filtering and Prediction Problems. *Journal of Basic Engineering*, 82(1):35–45, 03 1960.
- [32] Andrea Cavagna, Lorenzo Del Castello, Irene Giardina, Tomas Grigera, Asja Jelic, Stefania Melillo, Thierry Mora, Leonardo Parisi, Edmondo Silvestri, Massimiliano Viale, and Aleksandra M. Walczak. Flocking and turning: a new model for self-organized collective motion. *Journal of Statistical Physics*, 158(3):601–627, Feb 2015.
- [33] M. Ballerini, N. Cabibbo, R. Candelier, A. Cavagna, E. Cisbani, I. Giardina, V. Lecomte, A. Orlandi, G. Parisi, A. Procaccini, M. Viale, and V. Zdravkovic. Interaction ruling animal collective behavior depends on topological rather than metric distance: Evidence from a field study. *Proceedings of the National Academy of Sciences*, 105(4):1232–1237, 2008.
- [34] Tamás Vicsek, András Czirók, Eshel Ben-Jacob, Inon Cohen, and Ofer Shochet. Novel type of phase transition in a system of self-driven particles. *Phys. Rev. Lett.*, 75:1226–1229, Aug 1995.
- [35] IAIN D. COUZIN, JENS KRAUSE, RICHARD JAMES, GRAEME D. RUXTON, and NIGEL R. FRANKS. Collective memory and spatial sorting in animal groups. *Journal of Theoretical Biology*, 218(1):1–11, 2002.
- [36] Lucas Barberis and Fernando Peruani. Large-scale patterns in a minimal cognitive flocking model: Incidental leaders, nematic patterns, and aggregates. *Phys. Rev. Lett.*, 117:248001, Dec 2016.